ORIGINAL ARTICLE

Development of Network Topology and Functional Connectivity of the Prefrontal Cortex

Katherine C. Lopez[1],[*], Sridhar Kandala[2], Scott Marek[2], and Deanna M. Barch[1],[2],[3]

[1]Department of Psychological & Brain Sciences, Washington University, St Louis, 63130 MO, USA, [2]Department of Psychiatry, Washington University, St Louis, 63110 MO, USA and [3]Department of Radiology, Washington University, St Louis, 63110 MO, USA

[*]Address correspondence to Katherine C. Lopez, Department of Psychological & Brain Science, Washington University, One Brookings Drive St Louis, MO, USA. Email: lopezkc@wustl.edu

Abstract

The prefrontal cortex (PFC) comprises distinct regions and networks that vary in their trajectories across development. Further understanding these diverging trajectories may elucidate the neural mechanisms by which distinct PFC regions contribute to cognitive maturity. In particular, it remains unclear whether PFC regions of distinct network affiliations differ in topology and their relationship to cognition. We examined 615 individuals (8–21 years) to characterize age-related effects in participation coefficient of 28 PFC regions of distinct networks, evaluating connectivity profiles of each region to understand patterns influencing topological maturity. Findings revealed that PFC regions of attention, frontoparietal, and default mode networks (DMN) displayed varying rates of decline in participation coefficient with age, characterized by stronger connectivity with each PFC's respective network; suggesting that PFC regions largely aid network segregation. Conversely, PFC regions of the cinguloopercular/salience network increased in participation coefficient with age, marked by stronger between-network connections, suggesting that some PFC regions feature a distinctive ability to facilitate network integration. PFC topology of the DMN, in particular, predicted improvements in global cognition, including motor speed and higher order abilities. Together, these findings elucidate systematic differences in topology across PFC regions of different network affiliation, representing important neural signatures of typical brain development.

Key words: graph theory, hubs, large-scale networks

Introduction

The prefrontal cortex (PFC) is critical to an array of higher order cognitive functions that mature throughout development (Diamond 2009). Understanding how PFC maturity facilitates refinements in these cognitive abilities has been an area of ongoing research. There is abundant evidence that the PFC undergoes a protracted development from childhood into adulthood, with distinct regions displaying varied age-related changes in structure and function (Giedd et al. 1999; Luna et al. 2001; Tamm et al. 2002; Kanemura et al. 2003; Rubia et al. 2006). More recently, studies using resting state functional connectivity (RSFC) to examine the connections between brain regions at rest have established

that different PFC regions are affiliated with distinct large-scale networks (e.g., Power et al. 2010). Notably, these networks display diverging trajectories of connectivity throughout development (Marek et al. 2015), providing some suggestions that PFC regions might also vary in their connectivity trajectories, possibly on the basis of their network affiliation. While studies have begun to describe the developmental changes in connectivity of select PFC regions (e.g., ventromedial PFC; Gee et al. 2013), an important extension of this work will be to examine the ways in which PFC regions systematically differ in their connectivity trajectories and how these differences are related to diverse measures of cognition.

A body of primarily structural MRI studies have underscored the prolonged and mostly curvilinear development of the frontal lobe, with several metrics of gray matter showing peak growth in late childhood, followed by a decline throughout adolescence (Giedd et al. 1999; Tamnes et al. 2017). The PFC, in particular, shows the greatest growth spurt and most prolonged trajectory within the frontal lobe (Kanemura et al. 2003; Sowell 2004; Casey et al. 2005), with subsequent work bringing attention to notable differences in the shape and magnitude of change across general PFC areas (Gogtay et al. 2004; Spencer-Smith and Anderson 2009; Matsui et al. 2016). Much of this work has characterized differences among PFC regions in terms of their anatomical location (e.g., medial vs. lateral, dorsal vs. ventral). For example, whereas gray matter trajectories of dorsolateral (DLPFC) and dorsomedial PFC (DMPFC) areas follow an inverted U trajectory, peaking during early adolescence, more orbital PFC areas display modest changes across development (Matsui et al. 2016). Although many of these differences were based on anatomical subdivisions of the PFC known to contain regions of diverse functions (Cieslik et al. 2013), region-specific differences in PFC development have also emerged in work examining functionally distinct PFC regions. For example, findings from task-based fMRI suggest that certain regions of the DLPFC show increasing activation in response to various tasks of executive functioning with age whereas more medial PFC and ventral PFC regions display age-related decreases in activation in response to similar tasks (Bunge et al. 2002; Casey et al. 2005; Rubia et al. 2016).

This heterogeneity in PFC development can now be contextualized by evidence from RSFC studies, which increasingly suggest that functionally distinct PFC regions operate in tandem with different sets of brain regions to form dissociable large-scale networks (e.g., Bressler and Menon 2010; Power et al. 2011; Eickhoff et al. 2016). For example, the DLPFC (BA 46) serves as a key anchor to the frontoparietal network (FPN; Power et al. 2011; Marek and Dosenbach 2018), the VLPFC (BA 44/47) is more closely linked to the cinguloopercular/salience network (CO/SN; Sadaghiani and D'Esposito 2015) and other regions, such as the DMPFC (BA 8/9/10), anchor the default mode networks (DMN) (Raichle 2015). Should these networks develop differently, one might expect that PFC regions associated with distinct network membership would accordingly show differences in brain development. While structural and functional studies certainly describe heterogeneity in PFC development that is consistent with this hypothesis, determining whether PFC regions of separate network affiliations systematically differ in their connectivity trajectories has remained surprisingly understudied. Emerging work focused on mapping the development of large-scale networks, however, reveal important clues about this possibility.

As the brain matures, large-scale networks appear to show key differences in their organization (i.e., topology) and connectivity patterns (Satterthwaite et al. 2013a; Grayson and Fair 2017). Whereas most networks, including the FPN and DMN, become increasingly segregated with age by strengthening their within-network connections (e.g., Gu et al. 2015), other networks, such as the CO/SN, appear to integrate with other networks via stronger between-network connections (e.g., Marek et al. 2015). Consistent with the idea that networks support an array of cognitive processes—the FPN, CO/SN, and attention networks for control functions (Gratton et al. 2018b) and the DMN for introspective abilities (Raichle 2015)—developmental changes in network topology have been increasingly tied to improvements in cognitive performance (Marek et al. 2015; Baum et al. 2017). By

extension, a network's tendency to segregate or integrate with age may simultaneously inform the ways in which different PFC regions change over the course of development and how these PFC regions may relate to cognitive maturity.

One possibility is that PFC regions differ in their topological development on the basis of their network affiliation. If so, one might predict that PFC regions of the FPN (e.g., DLPFC, BA 46, 9, 10) would show age-related patterns of topology that mirror network-level segregation of the FPN (i.e., greater connections with other regions of the FPN), while PFC regions of the CO/SN (e.g., VLPFC, BA44, 47) would display age-related patterns that parallel of network-level integration of the CO/SN (i.e., greater connections with regions of other networks). Such findings may help clarify the role that PFC regions play in facilitating network maturity. However, should PFC trajectories diverge on the basis of their network membership, it remains unclear whether all PFC regions embedded within the same network would follow similar trajectories, such that all PFC regions belonging to the FPN, for example, display similar strengthening of within-network connections. Work examining the development of hubs—regions of relatively greater importance to its network—provide some evidence that hubs regions develop at differing rates from non-hub regions (Cao et al. 2014), particularly among frontal areas (Wu et al. 2013). Therefore, it is also possible that hub status contributes to meaningful differences in patterns of PFC development among regions embedded within the same network.

Another point of uncertainty is the extent to which differences in PFC topology development relates to cognitive maturity. This question is of particular interest given that the PFC has long been implicated in wide-ranging higher order processes, including executive functions (Wang et al. 2008; Diamond 2009), more fluid processes, such as reasoning abilities (Waltz et al. 1999; Krawczyk et al. 2011), and social processing (Wood et al. 2003; Bicks et al. 2015). Because many of these functions have also been increasingly tied to large-scale networks, there remains a need to better understand how PFC regions of distinct network affiliation may be differentially supporting cognitive maturity.

To address these questions, the present study focuses on 2 primary aims: (1) characterizing the topological development of PFC regions of distinct network membership from late childhood to early adulthood and (2) examining how individual differences in PFC topology are associated with cognitive performance. To this end, we applied graph theory techniques to RSFC data to evaluate age-related differences in participation coefficient of PFC regions of distinct networks. Participation coefficient is a measure of centrality that captures the relative number of within-network connections (reflecting segregation) and between-network connections (reflecting integration) for a given brain region. This metric has been used to examine network-level development (Fan et al. 2011; Marek et al. 2015; Meunier et al. 2009), facilitating comparisons between region-level and network-level topology. Based on previously reported network-level trajectories, we hypothesized that PFC regions of the FPN, attention networks, and DMN would show evidence of segregation (i.e., decreasing participation coefficient) with age, while regions affiliated with the CO/SN would show evidence of integration (i.e., increasing participation coefficient). For our second aim, we examined the extent to which individual differences in PFC topology predicted performance on measures of cognition, particularly those commonly associated with the PFC, including executive functioning, reasoning abilities, and

social cognition. We expected that trajectories of PFC regions in networks central to top-down control (i.e., FPN, attention networks, and CO/SN) would predict improved performance on cognitive measures.

Materials and Methods

Study Design

The two aims of the current study were examined in several steps, summarized in Figure 1. To examine developmental trajectories of PFC topology (aim 1), PFC regions affiliated with the dorsal attention (DAN), ventral attention (VAN), FPN, cingulo-opercular/salience (CO/SN), somatosensory, and DMN were modeled for linear and non-linear age-related effects of participation coefficient. Two subsequent analyses were conducted: (1) For each PFC region with significant effects for age, seed-based analyses were used to examine how variations in connectivity profiles might be contributing to age-related differences in PFC topology and (2) for all PFC regions embedded within a given network, relative hub status (i.e., level of participation coefficient for a region) were compared with determine whether PFC regions with significant age-related effects displayed overall greater hubness relative to regions with stable (null) trajectories. The goal of this latter analysis was to determine whether relative hubness played a role in driving age-related effects. Next, the contributions of PFC topology to cognitive development were examined in two ways. First, we examined how PFC topology of varying networks predicted performance on three domains of cognition commonly implicated in PFC functioning—executive control, complex cognition, and social cognition—and a less common function, namely motor speed, the latter examined to determine whether relationships to cognition were specific to higher order functioning. For PFC regions that predicted cognition, we subsequently examined the extent to which PFC topology mediated the relationship between age and cognitive performance.

Participants

The present study examined participants from the neuroimaging arm of the Philadelphia Neurodevelopmental Cohort, a large-scale study examining child brain and cognitive development in a cohort of 997 individuals ranging from 8 to 21 years of age (Sattherwhaite 2016). Due to missingness in data (missing age, $N = 16$) and exclusion based on image processing protocol ($N = 366$; see MRI Preprocessing), a final sample of 615 subjects was analyzed. Details on data acquisition—including recruitment procedures, study parameters (e.g., inclusion/exclusion criteria), behavioral assessment (e.g., clinical and cognitive measures), and imaging acquisition—can be found in Satterthwaite et al. 2016.

Cognitive Functioning

All participants completed the Penn Computerized Neurocognitive Battery, a collection of 14 tests assessing various domains of cognitive functioning with good test–retest reliability (Moore et al. 2015; Satterthwaite et al. 2016; Swagerman et al. 2016). Given the role of PFC in a number of higher order processes ranging from executive functioning to more socially based processing (e.g., Waltz et al. 1999; Wang et al. 2008; Diamond 2009; Krawczyk et al. 2011), the present study examined performance on cognitive tests within the domains of Executive Control, Complex

Cognition, and Social Cognition, as identified by previous factor analyses (Moore et al. 2015). Specifically, tasks assessing executive control included performance on the: (1) Letter N-Back, a measure of working memory (total correct responses to 0-, 1-, and 2-back trials); (2) Condition Exclusion Test, a measure of mental flexibility and set shifting (accuracy score); and (3) Continuous Performance Task, a measure of sustained attention (total correct response to number and letter trials). Complex cognition was examined via total correct responses on the: (1) Verbal Reasoning Test, a measure of the language-based reasoning; (2) Matrix Reasoning Test, a measure of perceptual reasoning abilities; and (3) Line Orientation Test, a measure of complex reasoning of spatial abilities. Measures of social cognition included (1) Emotion Identification Test, a measure of emotional facial recognition and (2) Emotion Differentiation Test, a measure of emotion intensity discrimination. Moreover, to confirm that associations between brain metrics and cognition performance were distinctively related to higher order abilities, and not better accounted for by more basic processes, such as motor speed, performance on the Finger Tapping Test in dominant and non-dominant hands were also examined. To examine overall domain performance, we created composites scores, in which scores of each subtest were z-scored and then averaged across subtests within the domains. This yielded a single overall composite measure of executive control, complex cognition, social cognition, and motor speed for each participant. Finally, performance on the Wide Range Assessment Test (WRAT; standard score) was used as a measure of estimated premorbid IQ.

Neuroimaging Acquisition

All participants completed a battery of neuroimaging scans (total time = ~50 min) on a Siemens 3-T TIM TRIO scanner at the University of Pennsylvania (See Satterthwaite et al. 2016 for a complete description of all imaging acquisition and parameter details). The present study examined a single RSFC scan (~6 min, 124 frames) and two task-based fMRI tasks—a N-Back (~10.6 min, 210 frames) and an emotion identification task (~11.6 min, 231 frames). All images were acquired using a gradient-echo, echo-planar imaging sequence sensitive to Blood oxygen level dependent (BOLD) contrast (T_{2^*}; TR = 3000 ms, TE = 32 ms, field of view = 192 mm, flip angle = 90°, matrix 64×64, 46 slices, voxel size = $3 \times 3 \times 3$ mm). Additionally, T_1-weighted structural images were acquired in the axial plane using a magnetization-prepared rapid-acquisition gradient-echo three-dimensional sequence (TR = 1810 ms, TE = 3.5 ms, flip angle = 180°, 160 slices, field of view = 192 mm, voxel size = $1 \times 1 \times 1$ mm). Task-evoked activations were regressed out from the two task-based scans to maximize the amount of available resting state data, a method contingent on findings suggesting that task-evoked activity can be superimposed, in an approximately linear fashion, to spontaneous resting state activity (Fox et al. 2006; Fox and Raichle 2007). Thus, the removal of task-based activity from spontaneous activity yields data with reasonable correspondences to continuous resting state data (Fair et al. 2007), an approach applied in past resting state work (Nakamura et al. 2009; Cole et al. 2014; Sheffield et al. 2015)

MRI Preprocessing

All resting-state and task-based scans for each participant underwent several preprocessing steps using in-house scripts
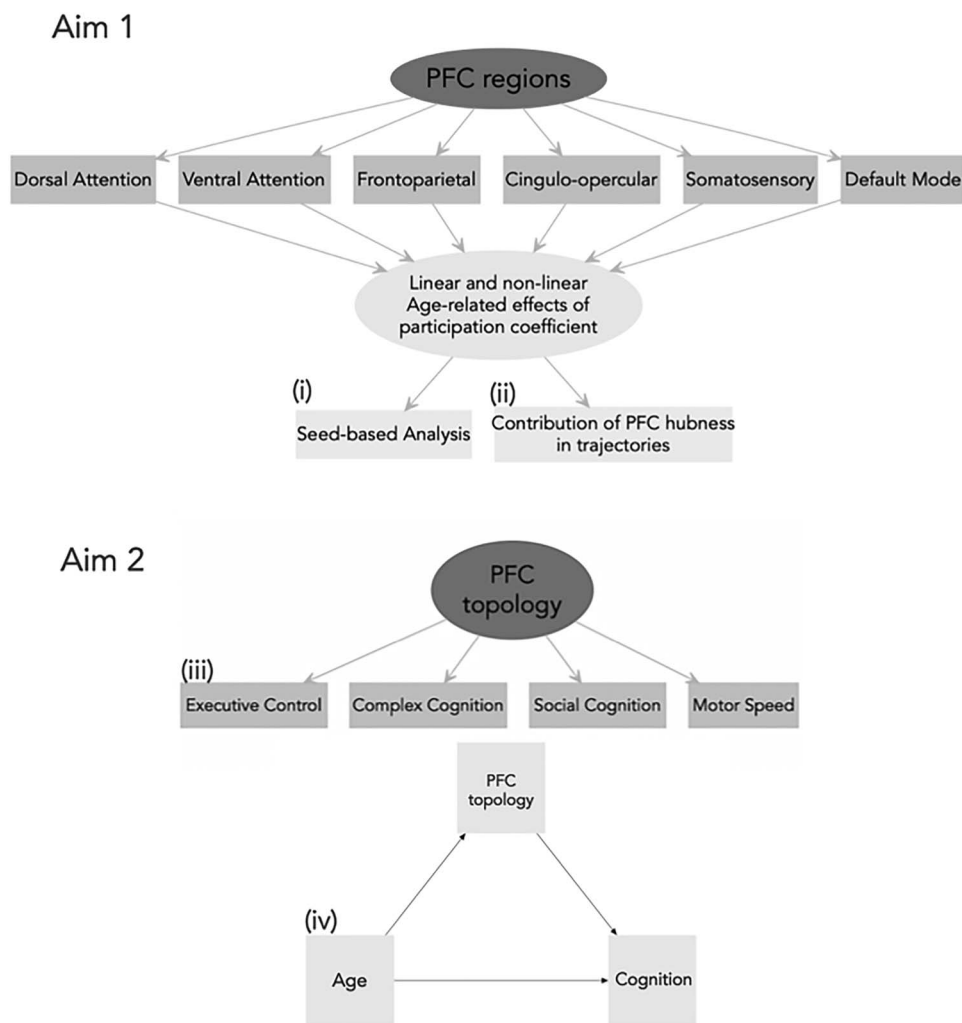
Figure 1. Study design. Aim 1: PFC regions of diverse networks were modeled for linear and non-linear effects of age of participation coefficient. Regions with significant age-related trajectories (i) underwent seed-based analysis to describe age-related changes in connectivity patterns; (ii) were compared with PFC regions of stable trajectories (i.e., no age effects) on the basis of relative hubness. Aim 2: regions with significant age-related trajectories were examined; (iii) in relation to performance on four domains of cognition; and (iv) as a mediator between age and cognitive functioning.

outlined in Power et al. (2014). These steps included: (1) image correction for slice-dependent time shifts (i.e., slice time correction); (2) correcting for odd/even slice intensity differences due to interpolated acquisition (i.e., debanding); (3) image spatial realignment within and across scans to reduce rigid body motion (i.e., motion correction); (4) scan intensity normalization to a whole-brain mode value of 1000 (i.e., variance normalization); (5) image registration of the T1 scan to an atlas template (WU 711-2B) in the Talairach coordinate system using a 12-parameter affine transform; (6) co-registration of the three-dimensional fMRI volume to the participant's T1 structural image; and (7) transformation of the fMRI data to $3 \times 3 \times 3$ mm voxel atlas space using a single affine 12-parameter transform (Ojemann et al. 1997). Additionally, structural T1× images were processed through Freesurfer (Fischl et al. 2002) to general subject-specific spatial masks for temporal signals from regions of non-interest (e.g., ventricles, white matter). After Freesurfer segmentation, voxels defined as white matter or lateral ventricles were selected as nuisance masks and eroded. The eroded masks were transformed to atlas space

and were overlaid on the T1w in atlas space and visually inspected to determine if there was gray-matter encroachment, or poor realignment to analysis space. If overlap problems were detected, and could not be fixed, the participant was excluded ($N = 25$). This inspection was conducted by a senior analyst (SK) with extensive experience in conducting quality control of this type for the Human Connectome Project. Participants were excluded for not acquiring three full functional scans ($N = 144$).

Functional Connectivity Processing

Additional processing steps were conducted on all scans using in-house software (Luking et al. 2011; Sylvester et al. 2013). First, scans with excess head motion artifacts were censored based on frame-wise displacement values greater than 0.2 mm, as previously described by Power et al. (2014). Next, data were demeaned and detrended within runs and then concatenated across runs (including both resting state and task) before nuisance time-series were regressed from the data. These nuisance regressors included 3 translation [X Y Z] and 3 rotation [P Ya R] measures,

their preceding time-points, and their squares, global signal (calculated as the average time-series across all voxels), white matter and cerebrospinal fluid time-series from Freesurfer-derived masks, and their first derivatives. For task scans, we treated the BOLD response as a superposition of the task activation and spontaneous BOLD data (Fox et al. 2006). A canonical hemodynamic response function and task activation was modeled as events convolved with a double-gamma response function and its first derivative, per task, to model the corresponding task (2 basis functions; Friston et al. 1998) as an additional nuisance regressor. Following this, censored time-points were replaced (interpolated) by least-squares spectral analysis of "good" time-points, a second-order Butterworth temporal band-pass filter ($0.009\ Hz < f < 0.08\ Hz$) was applied, and then spatial smoothing using a 6 mm full width at half maximum Gaussian kernel. Importantly, scan runs with less than 40 frames remaining after censoring ($X = 22$) and participants with less than 110 total frames remaining across all available runs were excluded from further analyses ($N = 44$).

Resting State FC Analyses

Functional subdivisions of the PFC were assessed using regions of interest (ROIs) from Power et al. (2011). The selection of ROIs was primarily guided by network membership, though an effort to achieve adequate coverage of the PFC was also made. Specifically, the PFC spans BA 6, 8, 9, 10, 11, 44, 45, 46, and 47, for a total of 67 ROIs (see Supplementary Table 1) that include the DAN (2 ROIs), VAN (3 ROIs), FPN (17 ROIs), cingulo-opercular/salience (13 ROIs), somatosensory (7 ROIs), DMN (20 ROIs), as well as, unassigned networks (5 ROIs). From these, at least two ROIs were selected per network, favoring ROIs that serve as canonical anchors to a given network. Pairs of ROI were homologs to the extent that contralateral ROIs were available in the Power atlas (e.g., DLPFC 101 and 104 of the DMN). Of note, the representation of ROIs of a given network was proportional to the overall size of network, with greater number of ROIs for networks of larger scale (e.g., default mode) and fewer ROIs for networks of smaller size (e.g., ventral attention). Spatial coverage of the PFC included lateral and medial regions of the dorsal, ventral, and orbital PFC. In total, 28 prefrontal ROIs were examined (see Table 1): 2 PFC regions of the DAN, 2 of the VAN, 4 of the FPN, 6 of the cingulo-opercular/salience network, 2 of the somatosensory network, 10 of the DMN, and 2 of an unassigned network. Of note, regions of cinguloopercular network and salience network were treated as a single network (i.e., CO/SN), given their high degree of functional overlap and ongoing discussions regarding whether these networks represent distinct components (Sadaghiani and D'Esposito 2015; Gratton et al. 2018b). All seeds were created using a 12 mm (diameter) spherical ROI using an in-house software (McAvoy et al. 2006) and based on the coordinates defined by Power et al. (2011). Table 1 contains information for all PFC seeds, including network affiliation, ROI number assigned by Power, Talairach coordinates, and Brodmann area.

Participation Coefficient Analysis

Functional networks were defined based on Power et al., 264 ROI atlas (total of 14 networks), which has previously been used to investigate graph characteristics over development (e.g., Marek et al. 2015). First, Pearson's r values were computed from the average BOLD time-series in each ROI and converted to Fisher's Z, yielding a 264 × 264 correlation matrix. BOLD pairwise corre-

lations (unweighted edges) were rank-ordered from strongest to weakest and thresholded based on a K density range of 1–10%, in 1% increments.

The purpose of this latter step was 3-fold: (1) to facilitate graph comparison across ages, given that graphs may exhibit differences in network density (i.e., distributions of correlation magnitude); (2) to retain the strongest correlations by eliminating connections (i.e., setting to $r = 0$) that fall below the threshold, thereby eliminating small correlations that may reflect noise; and (3) remove negative correlations (Powers 2010). Although there is no gold-standard procedure for density threshold range, 1–10% was chosen so as to be most consistent with previous literature that has identified and reproduced canonical large-scale brain networks at the strongest 10% densities (Yeo et al. 2011; Power et al. 2015). Using the brain connectivity toolbox (http://www.brain-connectivity-toolbox. net), measures of participation coefficient were computed. Specifically, participation coefficient represents the ratio of connections that a given node has to nodes of other networks (between-network connectivity) relative to its affiliated network (within-network connectivity; Rubinov and Sporns 2010). Lower values of participation coefficient (i.e., closer to 0) represent greater within-network connectivity and are suggestive of segregation, whereas higher values of participation coefficient (i.e., closer to 1) denote greater between-network connectivity and are reflective of network integration. Given our defined density range ($K = 1$–10%), our analysis yielded 10 graphs per node, per participant. As a final step, we averaged across densities, yielding a single average measure of participation coefficient per node, per participant. To confirm that sparsity of participation coefficient remained relatively stable across the 1–10% densities, we examined correlations between participation coefficient of all densities and age, as well as, correlations of graph metrics across all thresholds. The present study focused exclusively on graph metrics of the 28 PFC nodes selected a-priori.

Statistical Analyses

Modeling Age-related Differences in Participation Coefficient
Linear and non-linear age-related effects of PFC of participation coefficient were modeled using generalized additive models (GAM) with penalized splines (Wood 2017). Penalized splines introduce an optimal number of knots to the data in a data-driven fashion, with weights (i.e., penalties) placed onto each knot for rising levels of non-linearity (Baum et al. 2017). As such, penalized splines allowed for adequate smoothing of the data while averting under- or over-fitting data. This approach was particularly important for the current dataset, given that the tail end of our age distribution was susceptible to reduced statistical power due to significantly lower sample size among adults ranging from 19 to 21 years old (see Table 2 and Supplementary Fig. 1). Notably, mean framewise displacement (FD), numbers of frames retained, and sex were all used as covariates for each PFC region. Specifically, mean FD and numbers of frames retained were moderately correlated with age ($r = -0.28$ and $r = 0.31$, respectively, $P < 0.05$), suggesting that younger participants, on average, displayed greater movement (i.e., higher displacement) and retained fewer frames relative to older participants. To further control for movement, these parameters were used in all imaging analyses. The effects of sex were also controlled for to examine the overall trajectory in participation coefficient. However, given previous work demonstrating meaningful sex differences in brain development—particularly in

Table 1 ROI for the PFC

Associated network	PFC area	ROI #	X	Y	Z	BA
Dorsal attention	Dorsolateral	261	−32	−5	53	6
Dorsal attention	Dorsolateral	264	26	−9	54	6
Ventral attention	Ventrolateral	241	50	27	6	45
Ventral attention	Ventrolateral	242	−47	21	2	45
Frontoparietal	Dorsolateral	175	45	19	30	9
Frontoparietal	Dorsolateral	188	−41	33	24	46
Frontoparietal	Dorsolateral	201	−41	20	31	9
Frontoparietal	Ventrolateral	189	36	37	20	10
Cinguloopercular/salience	Dorsomedial	47	−4	−2	53	6
Cinguloopercular/salience	Dorsomedial	50	−17	−9	69	6
Cinguloopercular/salience	Dorsomedial	53	11	−6	69	6
Cinguloopercular/salience	Dorsomedial	54	5	3	51	6
Cinguloopercular/salience	Ventrolateral	207	45	17	14	44
Cinguloopercular/salience	Ventrolateral	220	−38	45	21	10
Sensory/somatomotor	Dorsomedial	17	−8	−24	63	6
Sensory/somatomotor	Dorsomedial	31	8	−21	72	6
Default mode	Dorsolateral	101	20	33	42	8
Default mode	Dorsolateral	104	−20	39	42	8
Default mode	Dorsomedial	99	−17	23	54	8
Default mode	Dorsomedial	102	11	48	42	8
Default mode	Dorsomedial	103	−11	48	42	8
Default mode	Dorsomedial	105	5	48	21	9
Default mode	Dorsomedial	115	−8	42	27	9
Default mode	Dorsomedial	121	11	24	60	6
Default mode	Orbitolateral	137	−44	27	−9	47
Default mode	Orbitolateral	139	47	30	−6	47
Unassigned	Orbitomedial	3	23	27	−12	11
Unassigned	Orbitomedial	182	−20	36	−15	11

Note. ROI's are based on Power et al. (2010) atlas, using Tailarach coordinates.

network-level trajectories of participation coefficient (Satterth-waite et al. 2015)—follow-up analyses were conducted for PFC regions with significant age-related effects to examine whether significant sex differences in trajectories emerged. Finally, to protect against type I errors, False Discovery Rate (FDR) was applied to correct for the number of analyses conducted. Moving forward, only FDR-corrected PFC regions whose participation coefficients were significantly predicted by age were subsequently analyzed for: (1) functional connectivity patterns (i.e., seed-based analyses) and (2) relationship to cognitive outcomes. These analyses were conducted in R.

Within-network PFC Comparison of Hub Status
As will be discussed below, age-related effects of PFC topology were not observed for all PFC regions belonging to the same network. Within a given network, some PFC regions showed age-related effects, while others remain stable throughout development. As a subsequent step, we examined whether overall hub status distinguished PFC regions with age-related effects from regions with stable trajectories. However, because participation coefficient is shown to change with age, we utilized estimates of participation coefficient (for each PFC seed) from a separate sample of adults, derived from Power et al. (2013), so as to examine topology estimates that were unbiased by the age-related variation in the current sample. On this Powers dataset from adults, we conducted an ANOVA on participation coefficient with region as the replication factor, and network and age effect (yes vs. no) as factors of interest. Analyses were controlled for the effects of mean FD, numbers of frames retained, and sex.

Table 2 Demographic information and cognitive outcomes

N	615
Age	14.57 (3.24)
Sex	F = 328, M = 287
IQ-Wrat (standard score)	102.12 (15.99)
Ethnicity	
Caucasian	289
Black	254
Other	10
Multi-racial	58
Executive function	
N-back total correct	27.66 (2.69)
Condition exclusion task	1.97(0.70)
CPT total correct	51.82 (7.98)
Complex cognition	
Verbal reasoning total correct	11.13 (2.72)
Matrix reasoning total correct	11.76 (4.09)
Line orientation total correct	8.98 (4.10)
Social cognition	
Emotion identification total correct	33.48 (3.07)
Emotion differentiation total correct	29.23 (7.96)

Data are presented as mean (SD).

Seed-based Models
We conducted follow-up seed-based analyses to illustrate the patterns of functional connectivity that were contributing to age-related effects in participation coefficient. Given that these

regions were selected a-priori based on preceding modeling of age-related effects in participation coefficient, all seed-based analyses in the current study are not statistically independent and thus are regarded as descriptive.

For each PFC region, average BOLD time-series were correlated with BOLD signal of every other voxel in the brain (i.e., ROI-voxel analysis) and subsequently converted into Fisher's R to Z transforms. To correct for multiple comparisons, we used AFNI's 3dclustsim (Cox et al. 2017) to apply a cluster threshold size of 30.6 continuous voxels with faces touching (i.e., bi-sided, first nearest neighbor clustering) that was determined based on voxel-level threshold of $P < 0.001$ and a whole brain level threshold of $\alpha < 0.05$. Regressions for our seed-based analysis included age as our primary predictor, and three covariates: sex, mean FD, and numbers of frames retained. Then, we color-coded all identified clusters based on its network affiliation using the Power atlas. Specifically, we binarized each map, and calculated the Sorensen-Dice coefficient for the positive clusters and negative clusters, separately, to a voxel-wise Power network map (Power and Petersen 2013). Each cluster was assigned to the Power network with the highest Sorenson-Dice coefficient. These analyses were performed in MATLAB.

Relationship between PFC Topology and Cognitive Functioning
First, we examined the developmental trajectories of 4 domains of cognition, modeling linear and non-linear age-related effects of Executive Functioning, Complex Cognition, Social Cognition, and Motor Speed performance. These were also modeled via GAM with penalized splines. Second, linear models were used to examine whether participation coefficient predicted each cognitive outcome. For these analyses, the following variables were used as covariates: mean FD, number of frames retained, sex, age, and IQ (i.e., WRAT, Standard Score). Finally, for all PFC regions predicting cognition, we conducted mediation analyses to determine whether participation coefficient of PFC regions mediated the relationship between age and cognition using the Lavaan package in R (Rosseel 2012) and bootstrapping ($n = 1000$).

Results

Demographic Characteristics

Table 2 includes a summary of participant's demographic characteristics and performance on cognitive tasks.

Participation Coefficient Results

Findings are organized based on a PFC region's associated network, identifying a PFC region by its location and the ROI number assigned by Power et al. (2011) (e.g., DLPFC 261). Figure 2 depicts all significant (FDR corrected) age-related effects of PFC regions for each network and Supplementary Table 2 provides presents all relevant data of these trajectories. Overall, PFC regions affiliated with the DAN, VAN, FPN, and DMN displayed varying rates of age-related decline in participation coefficient. In particular, a DLPFC region of the DAN (Fig. 2A, green trajectory; $R^2 = 0.034$) displayed a curvilinear decline in participation coefficient throughout late childhood into adolescence, while a VLPFC of the VAN (Fig. 2A, cyan trajectory; $R^2 = 0.034$) displayed a linear decline as a function of age. Two DLPFC regions of the FPN (Fig. 2B, yellow trajectories; both $R^2 = 0.039$) also

displayed non-linear decreases in participation coefficient throughout development, while PFC regions of the DMN (Fig. 2D, red trajectories, R^2 ranged from 0.034 to 0.098) exhibited a combination of linear and curvilinear declines with age. Of these trajectories, significant sex by age interactions was observed for a DLPFC (261) region of the DAN and a DLPFC (188) region of the FPN. For both regions, declines in participation coefficient were present in females ($p^{DLPFC(261)} = 0.000$; $p^{DLPFC(188)} = 0.029$) and not males ($p^{DLPFC\ 261} = 0.872$; $p^{DLPFC(188)} = 0.998$; see Fig. 2). Finally, 2 regions associated with the CO/SN—a VLPFC and a DMPFC region (Fig. 2C, purple trajectories; $R^2 = 0.034$ and $R^2 = 0.026$, respectively)—showed increases in participation coefficient with age. Where the VLPFC shows a non-linear increase from childhood to adolescence, the DMPFC increased linearly as a function of age.

Notably, these trajectories reflected age-related effects of participation coefficient measurements that were averaged across densities (i.e., $K = 1$–10%). To ensure that each PFC's trajectory were not greatly impacted by the sparsity of thresholds (i.e., age-related effects held across densities), participation coefficient at each K density was correlated with one another, the overall mean K density, and age, for every PFC region displaying significant age-related effects. As shown in Supplementary Figure 2, for each PFC region, participation coefficient measurements across densities were positively correlated with one another, such that participation coefficient of adjacent densities displayed highest correlations. Mean K density (i.e., our primary outcome measure) also showed moderate to high correlations with each individual density. Importantly, both individual densities ($K = 1$–10%) and overall mean density displayed the expected patterns of associations with age. Specifically, for all PFC regions displaying average declines in participation coefficient (i.e., PFC regions of the DAN, VAN, FPN, and DMN), participation coefficient at each density 1–10% showed the expected negative correlation with age. Conversely, for all PFC regions displaying average increases in participation coefficient (i.e., PFC regions of the CO/SN), participation coefficient at each densities display positive associations with age. Supplementary Figure 3 illustrates means and standard deviation of participation coefficient for each density and overall mean density. Here, an important observation is that rank order across PFC regions is preserved irrespective of density. For example, participation coefficient for DLPFC (201) at threshold = 1–10 was consistently higher than participation coefficient for DMPFC (102) at threshold = 1–10. All together, these patterns provide evidence for fairly stable participation coefficient across thresholds.

To confirm that temporal signal to noise ratio (tSNR) of an ROI did not influence age-related differences in participation coefficient, tSNR was regressed onto age for each of the 12 ROI that showed an age-related effect. As expected, findings failed to show a significant relationship between tSNR and age (all $P > 0.05$), indicating the developmental changes observed for each ROI are unrelated to SNR.

Finally, we conducted additional analyses to examine whether overall PFC trajectories of participation coefficient for a given network replicated network-level trajectories of topology previously reported in Marek et al. (2015). To this end, participation coefficients for all PFC regions within a network (i.e., with and without age-related effects) were averaged to obtain a single metric of participation coefficient for each network. We then modeled these network measures with
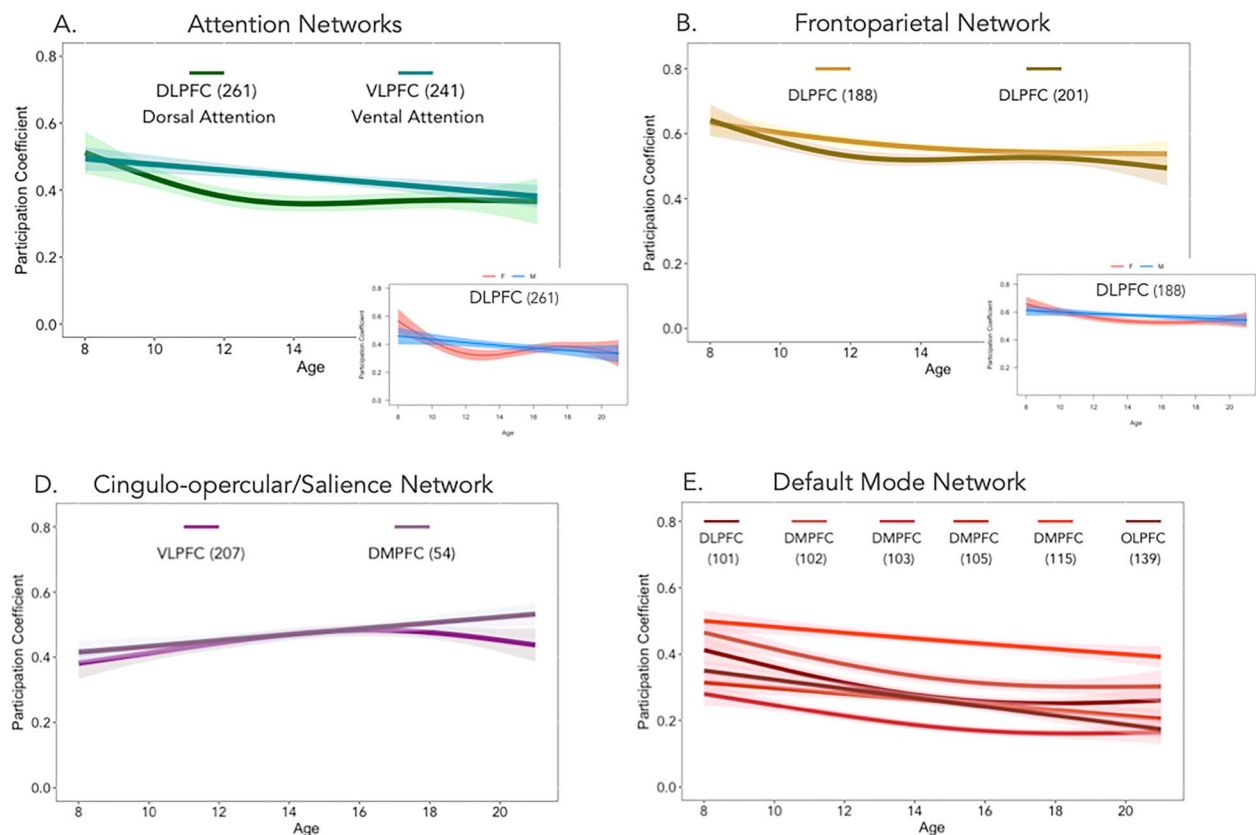
Figure 2. Topological trajectories of PFC regions affiliated with distinct networks. Age-related effects were observed for PFC regions affiliated with (*A*) attention networks, (*B*) FPN, (*C*) CO/SN, and (*D*) DMN. For each network, PFC regions displayed similar patterns of age-related effects. Sex differences were observed for 2 PFC regions of the DAN and FPN, in which females showed curvilinear declines in participation coefficient with age while males did not. Data are corrected for motion parameters (i.e., FD and numbers of frames retained).

penalized splines to examine for linear and non-linear effects of age. As shown in Supplementary Figure 4, overall participation coefficient of the FPN and DMN displayed curvilinear decreases from late childhood into early adulthood (Supplementary Fig. 4C,E, respectively), similar to network-level decreases observed in Marek (2015) (Supplementary Fig. 4F; yellow and red trajectories, respectively). Our findings also show that both DAN and VAN (Supplementary Fig. 4A,B; green and teal trajectories, respectively), not previously examined in Marek et al., also display varying rates of declines in participation coefficient with age. However, in contrast to Marek (2015), our findings failed to reveal significant age-related increases in overall participation coefficient of CO/SN, though an upward slope was noted (Supplementary Fig. 4D). It is worth noting that CO/SN increases in participation coefficient, observed in Marek (2015) (Fig. 4F; gray trajectory), were largely driven by subcortical regions, including insular regions that are anatomically adjacent to the VLPFC region that did exhibit significant age-related increases in participation coefficient. Overall, using a separate dataset with a larger sample than Marek et al., our findings mostly replicate previously reported network-level age-related changes in participation coefficient throughout development, though effects in the current findings are smaller in magnitude and span a slightly different age range (8–21 years old in our sample, compared with 10–26 years old in Marek's (2015) sample.

Within-network PFC Comparisons of Relative Hubness (i.e., Average Participation Coefficient)

Thus far, our findings suggest that certain PFC regions within a network display age-related effects while other regions of the same network remain stable. Leveraging off prior work suggesting that hub regions develop at differing rates from non-hub regions (Cao et al. 2014), particularly among frontal areas (Wu et al. 2013), we examined whether relative hub status distinguished PFC regions with age-related effects from regions with stable trajectories (i.e., no age-related effect) using the data from the 120 adults in Powers et al. Supplementary Figure 5 depicts participation coefficient estimates for PFC regions of the DAN, VAN, FPN, CO/SN, and DMN. Note that 4 ROIs were not examined—2 ROIs of the somatosensory networks and 2 ROIs of an unassigned network—due to overall non-significant PFC trajectories within a network. There was a significant main effect of network ($F_{(4,14)} = 18.013$, $P < 0.001$), with post hoc analyses indicating significantly lower participation coefficient in DMN compared with all other networks, and in the DAN compared with FPN. However, there was no significant main effect of age pattern ($F_{(1,14)} = 0.626$, $P < 0.442$), and no significant interaction between network and age pattern ($F_{(4,14)} = 1.008$, $p < 0.436$). We obtained the similar findings of no significant differences as a function of age when computing average participation coefficient for each individual ROI in the current dataset (see Supplementary Table 4)

Seed-based Analysis: Connectivity Profiles Characterizing Changes in PFC Topology

The age-related effects we observed for some PFC regions suggest that connectivity between a given PFC seed and nodes of other networks differs with age. To better understand the connectivity profiles contributing to developmental differences in PFC topology, we conducted additional analyses to examine age-related effects of connectivity patterns. As with results presented above, PFC regions were grouped based on their network affiliation (i.e., control vs. DMN).

PFC Regions Associated with Control networks

Figure 3 illustrates seed-based RSFC patterns for PFC regions associated with control networks. For PFC regions of attention networks, a DLPFC of the DAN showed nonlinear decreases in participation coefficient, while the VLPFC of the VAN showed linear declines with age. Seed-based analyses indicate that the DLPFC of the DAN displays increasing connectivity with its own network (i.e., DAN), regions of the somatosensory network, and concurrent decreasing connectivity with the DMN (Fig. 3A). Similarly, the VLPFC of the VAN demonstrated increasing connectivity with its own network (i.e., VAN), a few regions of the visual network, and decreasing connectivity with regions of the default mode, DAN, and somatosensory networks (Fig. 3B). Together, these profiles highlight stronger within-network connections and reductions in between-network connections with several networks (especially the DMN) that appear to concurrently contribute to declines in participation coefficient.

Two DLPFC regions affiliated with the FPN showed curvilinear declines in participation coefficient, with some variability in their rate of decline. Seed-based analyses indicate that the DLPFC (201) region, positioned posteriorly within BA 9, showed decreasing connectivity with regions comprising the CO/SN and auditory networks (Fig. 3C). In contrast, the DLPFC (188), positioned anteriorly within BA 46, displayed a dual profiles of (1) increasing connectivity with its own network, the FPN, and regions of the VAN, as well as; (2) decreasing connectivity with several structures of the CO/SN, somatosensory, and auditory networks. Jointly, these profiles suggest that declines in participation coefficient of both DLPFC regions are primarily reflecting decreasing connectivity with the CO/SN, with connectivity differences to other networks (FPN and VAN) likely contributing to slight differences in rate of participation coefficient decline (i.e., slope) across DLPFC regions.

Two PFC regions of the CO/SN showed increases in participation coefficient—a VLPFC, which showed curvilinear increases in participation coefficient, and a DMPFC, displaying linear increases with age. Seed-based analyses for both regions showed increasing connectivity with several cross networks (Fig. 3E,F); the VLPFC with the FPN, VAN, and DAN and the DMPFC with its own network—the CO/SN—and somatosensory networks. Both PFC regions also displayed decreasing connectivity with varying portions of the DMN. Together, these profiles suggest that increasing between-network connectivity with various networks—both control and sensory networks—contribute to increases in participation coefficient of PFC region of the CO/SN throughout adolescence.

PFC Regions Associated with the DMN

PFC regions affiliated with the DMN, including 4 DMPFC regions, 2 DLPFC regions and an OLPFC region, all showed decreasing participation coefficient of varying rates from late childhood to adolescence and displayed a number of similarities in their RSFC profiles (see Fig. 4). First, all PFC regions showed increasing connectivity with varying portions of their affiliated network, the DMN, as a function of age. A minority of regions displayed increased connectivity with the somatosensory network (i.e., 2 right DMPFC regions). Nearly all PFC regions also demonstrated decreasing connectivity with structures of the CO/SN (except the OLPFC) and a number of regions displayed additional decreasing connectivity with portions of the DAN and somatosensory networks. Overall, PFC regions of the DMN showed greater within-network connectivity and decreasing between-network connectivity, primarily the CO/SN, with variability in connectivity profiles with other cross networks, potentially accounting for differences in linear versus non-linear downward slopes.

Relationships to Cognitive Function

Relationships between participation coefficients of PFC regions and cognitive functioning were assessed in three ways: (1) mapping the developmental trajectories of higher order cognitive functioning, including executive functioning, complex cognition, social cognition, and more basic processing, namely motor speed; (2) examining whether participation coefficient predicted these domains of cognition; and lastly (3) examining whether participation coefficient of PFC regions mediated the relationship between age and cognitive performance. Cognitive domains were modestly correlated with one another (see Fig. 5A) and associations between individual tests ranged from small to moderate (see Supplementary Fig. 6).

For the first set of analyses (Fig. 5B), findings revealed that executive control increased linearly with age ($P = 0.00$, $R^2 = 0.24$), whereas complex cognition, social cognition, and motor speed increased in a curvilinear fashion as a function of age (complex cognition: $P = 0.00$, $R^2 = 0.44$; social cognition: $P = 0.00$, $R^2 = 0.28$; motor speed: $P = 0.00$, $R^2 = 0.34$). Lower participation coefficient of PFC regions of the DMN predicted better performance across all cognitive measures, as well as motor speed. Specifically, DMPFC (103) predicted higher executive control ($R^2 = 0.15$); DMPFC (103) and DLPFC (101) regions were associated with better performance in measures of Complex Cognition ($R^2 = 0.31$ for both regions); and DMPFC (103), DLPFC (101), and OLPFC (139) predicted higher social cognition performance (R^2 ranged from 0.06 to 0.07). Finally, DMPFC (103), DMPFC (102), DMPFC (101), and OLPFC (139) predicted higher motor performance ($R^2 = 0.08$–0.10). Although participation coefficient of the DLPFC (188) of the FPN and DLPFC (261) of the DAN predicted better performance on measures of executive control ($R^2 = 0.142$ for both regions), these relationships did not pass FDR correction. See Supplementary Table 3 for a comprehensive summary of all PFC-cognition relationships, including associations that did not survive FDR correction. Finally, despite significant associations of age and PFC participation coefficient with cognitive performance, none of the three PFC regions of DMN mediated the relationship between age and cognition (P's: 0.28–0.93). Supplementary Figure 7 summarizes direct and indirect data for all mediation analyses.

Discussion

Using a combination of graph theory and seed-based analyses, we examined age-related differences in PFC topology from late childhood to early adulthood. Our findings revealed that PFC regions of the DAN, VAN, FPN, and DMN displayed varying rates of age-related decreases in participation coefficient. These
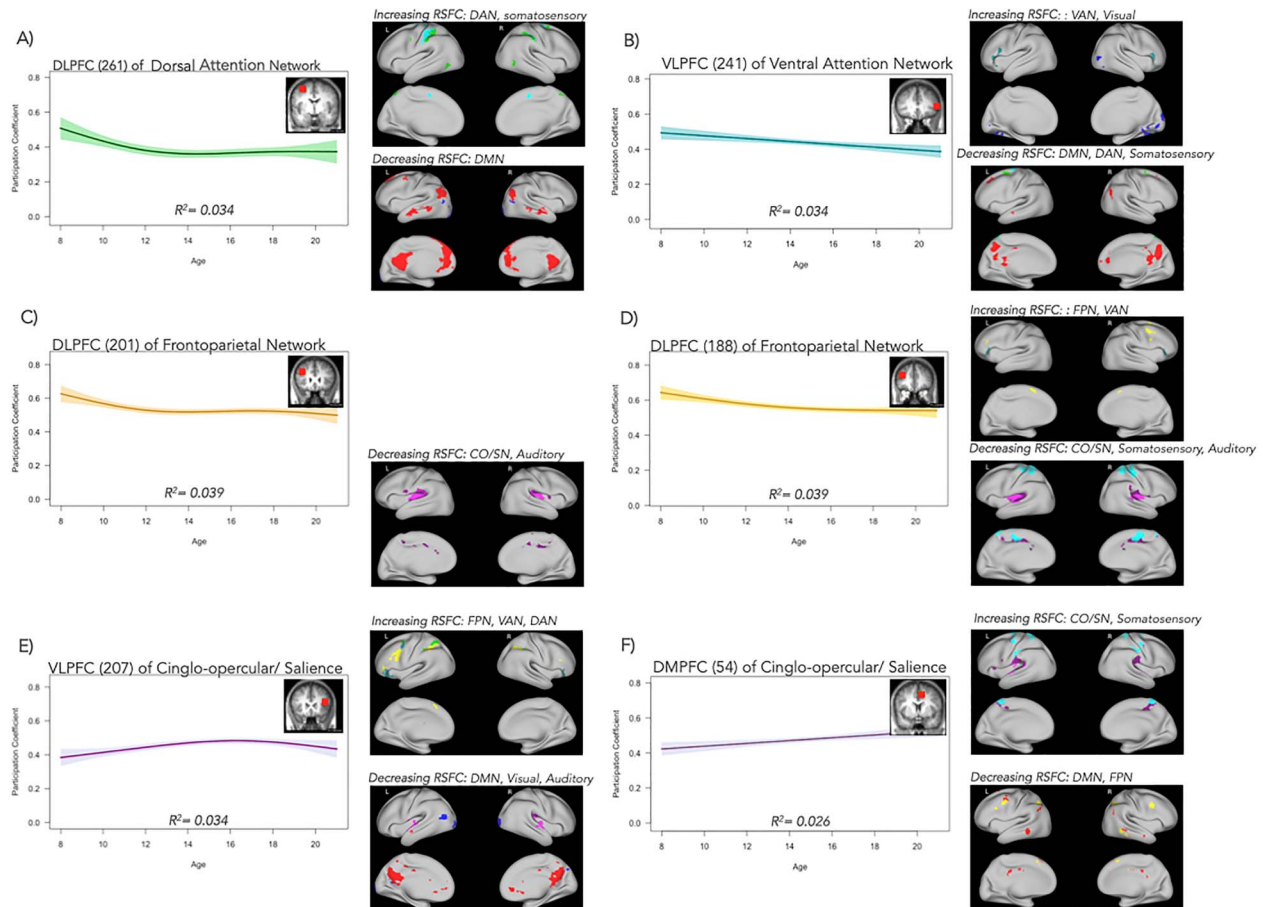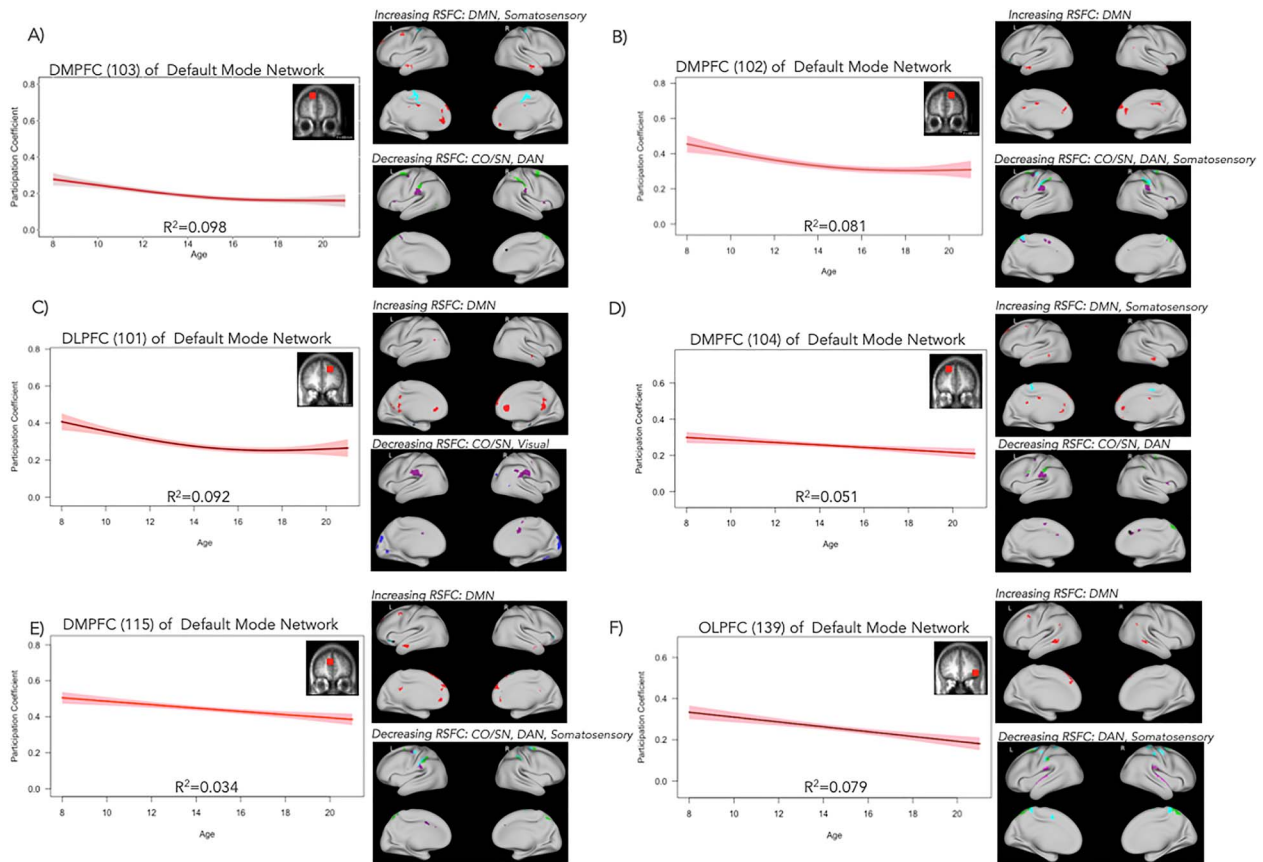
Figure 3. Topological trajectories of PFC regions affiliated with control networks. Age-related declines in participation coefficient were observed for the (A) DLPFC of the DAN; (B) VLPFC of the VAN; (C) a DLPFC of the FPN, positioned within BA 9; and (D) a canonical DLPFC of the FPN, embedded within BA46. For all these PFC regions, seed maps (located to the right of each graph) illustrate that age-related decreases in participation coefficient were generally characterized by increasing connectivity with each region's respective network and decreasing connectivity with cross networks. In contrast, 2 PFC regions of the CO/SN—(E) a VLPFC and (F) a DMPFC—displayed age-related increases in participation coefficient. Seed maps for each region primarily revealed increasing connectivity with a number of cross-network, including control and sensory networks. Of note, identified clusters are color-coded based on network affiliation assigned by Power et al. (2010): DAN (green); VAN (teal); FPN (yellow); cingulo-opercular/salience (purple); visual (blue), auditory (pink), somatosensory (cyan).

declines generally reflected (1) increased connectivity with each PFC's respective network and (2) decreased connectivity with an array of other networks. Jointly, these profiles suggest that most PFC regions show patterns of increasing network segregation with age, such that each PFC region becomes more modular with its respective network. In contrast, two regions of the CO/SN displayed increases in participation coefficient across development, reflecting primarily stronger between network connectivity with the control and sensory networks. These profiles indicate that PFC regions affiliated with the CO/SN exhibit distinctive patterns of network integration, whereby the regions of CO/SN interact with other networks into adolescence. Notably, these age-related differences in PFC display striking similarities to network-level trajectories of topology reported for control and DMN (e.g., Marek et al. 2015), suggesting that PFC regions systematically differ in their topological trajectories, largely on the basis of their network affiliation.

Prefrontal Regions of Control Networks

DLPFC regions of the DAN and FPN and a VLPFC of the VAN displayed overall descending trajectories of participation

coefficient across development. Interestingly, regions of the DAN and FPN showed similar rates of accelerated declines in participation coefficient during early childhood, with most regions plateauing around 14–15 years old. Given close functional relationships between the DAN and FPN, it is not entirely surprising that these regions would display comparable trajectories in topology across development. Indeed, there is evidence that these networks form part of a larger "dorso-fronto-parietal" system that supports attentional control (Szczepanski et al. 2013; Vossel et al. 2014; Ptak et al. 2017), with close interconnectivity noted between the DAN and FPN (Spreng et al. 2013) and even some suggestions that the DAN may be one (of several) sub-systems of the FPN (Dixon et al. 2018). Females, in particular, appeared to drive the age-related effects for the DLPFC of the DAN and a canonical DLPFC of the FPN (i.e., embedded within 46). Together, these trajectories bear a close resemblance to curvilinear decreases in network-level participation coefficient of the FPN during early adolescence (Marek et al. 2015), and, more generally, parallel the timelines of structural and functional change reported for various DLPFC regions (e.g., Ordaz et al. 2013; Matsui et al. 2016). The VLPFC of the VAN, in contrast, showed more of a steady and prolonged

Figure 4. Topological trajectories of PFC regions affiliated with the DMN. Age-related declines in participation coefficient were observed for four DMPFC regions (A, B, D, E), a DLPFC region (C), and an OLPFC region (F) of the DMN. For all PFC regions, seed maps (located to the right of each graph) illustrate that age-related decreases in participation coefficient were generally characterized by increasing connectivity with varying portions of the DMN (i.e., within-network connectivity) and decreasing connectivity with cross networks, primarily the DAN and cingulo-opercular/salience networks Notably, identified clusters are color-coded based on network affiliation assigned by Power et al. (2010): DAN (green); VAN (teal); FPN (yellow); cingulo-opercular/salience (purple); visual (blue), auditory (pink), somatosensory (cyan).

decline in participation coefficient from childhood into early adulthood. Although network-level participation coefficient of the VAN has not been previously directly examined, the somewhat diverging trajectories observed between PFC regions of the DAN and VAN may be related to the different aspects of attention these networks subserve—the DAN in top-down attention control (e.g., selective attention) and the VAN in bottom-up attention processing (Vossel et al. 2014)—functions that may develop at slightly varying rates over the course of development.

These overall patterns of topology suggest that PFC regions of most control networks would largely be involved in establishing within-network connections. Indeed, connectivity profiles examined for all PFC regions revealed increasingly positive within-network connectivity with each PFC's respective network (i.e., DAN, FPN, and VAN), patterns corroborating previous reports of age-related increases in within-network connectivity of the DAN and FPN (Sherman et al. 2014; Farrant and Uddin 2015). These regions also displayed concurrent negative connectivity with other networks. Specifically, the DLPFC of the DAN showed decreasing connectivity with the DMN with age, coming to resemble adult-like anti-correlations between the DAN and DMN (Spreng et al. 2013; Petrican et al. 2017). Regions of the FPN and the VAN, on the other hand, showed decreasing connectivity with the CO/SN to varying degrees, such that

regions with accelerated declines in participation coefficient (i.e., DLPFC of the FPN) displayed negative connectivity with a greater number of CO/SN regions than regions with more steady linear declines (i.e., VLPFC of the VAN). Despite some variability in the extent of connectivity, these findings are collectively in good agreement with reports of negative connectivity between the CO/SN and both the FPN (Gratton et al. 2018b) and VAN (Farrant and Uddin 2015) in adulthood. Overall, patterns of increasing within-network connections and decreasing between-network connections appears to simultaneously contribute to topological declines in participation coefficient, consistent with the idea that PFC regions of the DAN, VAN, and FPN play a role in facilitating network-level segregation across development.

One likely purpose for PFC regions to consolidate within-network connections, rather than acquire cross-network links, may be to assist in the fine-tuning of specialized functions of networks by way of separating processing of different modalities. More specifically, the DAN is implicated in endogenous alerting and orienting attention (e.g., Petersen and Posner 2012), functions known to emerge earlier during childhood (Posner et al. 2013). In our dataset, childhood was marked by prominent declines in participation coefficient for the DLPFC of the DAN, representing one possible neural signal of DAN segregation needed to support the early maturation of attentional processes.
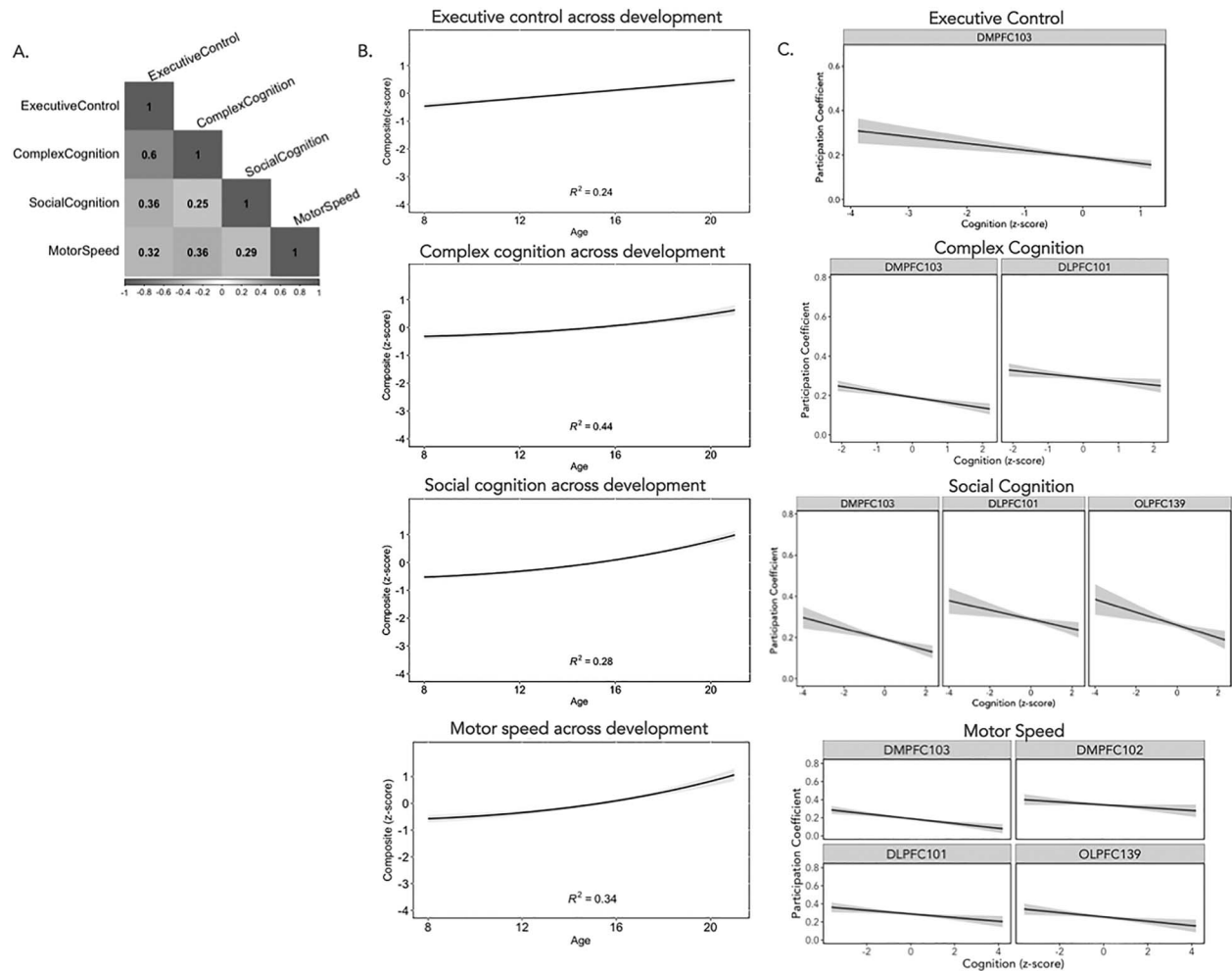
Figure 5. PFC topology in relation to cognitive performance. (A) Associations between executive control, complex cognition, social cognition, and motor speed ranged from small to moderate, suggesting that these domains of cognition can be considered separable but related to one another. (B) All four domains of cognition improve with age and (C) are predicted by decreasing participation coefficient (i.e., segregation) of several PFC regions affiliated the DMN, suggesting that age-related segregation of the DMN might support general cognitive processing.

The FPN, on the other hand, is involved in the initiation and moment-to-moment adjustment of control (Dosenbach et al. 2007; Marek and Dosenbach 2018) important for the execution of executive functions (Wallis et al. 2015) that are noted to mature in a more protracted manner, extending into early adulthood (Tamm et al. 2002; Velanova et al. 2008). Accordingly, 2 DLPFC regions of the FPN appear to contribute to a protracted pattern of FPN segregation, with a more canonical DLPFC region of the FPN embedded within BA46 showing patterns of segregation extending into later adolescence (17–18 years old). These DLPFC regions, alongside other critical regions of the FPN, may jointly support protracted refinements in executive abilities. Females, in particular, display these patterns of segregation for the DAN and partly for the FPN, consistent with evidence that females display greater patterns of within-network connectivity throughout development (Satterthwaite et al. 2015), perhaps suggesting that females may reach maturity for attention and executive processing at earlier periods of development than males. Finally, the VAN, which is largely right lateralized, is thought to play a role in reorienting of attention to behaviorally relevant stimuli (Corbetta and Shulman 2002). The ability to

focus attention, particularly under high cognitive load (Todd et al. 2005), is thought to be supported, in part, by adequate suppression of the VAN (Vossel et al. 2014). Increasing segregation of the VAN may, therefore, facilitate mature top-down driven attention. In line with this hypothesis, our findings show that a right VLPFC displayed evidence of VAN segregation, occurring in a linear and prolonged fashion, possibly supporting more effective attention control into adulthood. In short, trajectories of PFC topology and connectivity, which collectively appear to facilitate network-level segregation, may be important in refining cognitive abilities these networks are thought to subserve.

Two PFC regions of the CO/SN also displayed age-related effects in topology. However, unlike previous control-affiliated regions, those belonging to the CO/SN demonstrated increases in participation coefficient from childhood to adolescence. Specifically, a VLPFC region showed prominent curvilinear increases from around 13 years old into adulthood while a DMPFC region increased steadily with age. These trajectories are in agreement with growing evidence of network-level integration of the CO/SN (Grayson et al. 2014; Marek et al. 2015; Mohr et al. 2016) and suggest that these PFC regions may

play a distinctive role in forming between-network connections throughout development. Consistent with this line of thought, connectivity profiles reveal patterns of network integration for both regions. In particular, the VLPFC showed increasing between-network connectivity with several control networks, including the FPN and attention networks, a notable finding given that the CO/SN has been reported to work in parallel with the FPN to support top-down control in adulthood (Dosenbach et al. 2008). Relative to the FPN's role in moment-to-moment adjustment, the CO/SN is thought to be involved in task maintenance. Coordinated activity between the CO/SN and other control networks over the course of development may, therefore, promote the combination of different types of attentional processes and moment-to-moment corrective adjustments to meet increasingly complex goal-directed demands, such as executive abilities, known to improve markedly throughout adolescence (Tamm et al. 2002; Diamond 2012; Lee et al. 2013).

Prefrontal Regions of the DMN

A number of PFC regions affiliated with the DMN, including DMPFC, DLPFC, and OLPFC regions, displayed overall declines in participation coefficient throughout development. Whereas some regions showed precipitous declines, beginning around 12 years and plateauing around early adulthood, other regions displayed steady decreases into adulthood. Overall, these regional trajectories displayed a strong resemblance to network-level decreases in participation coefficient of the DMN (Marek et al. 2015) and suggest that PFC regions also play a role in facilitating DMN segregation. Connectivity patterns suggest that most PFC regions contribute to DMN segregation by increasing connectivity with varying portions of the DMN and decreasing connectivity primarily with the DAN and CO/SN. These connectivity profiles are not only consistent with typical patterns of anti-correlations between task-negative and task-positive (control) networks at large, they are also in agreement with cross-sectional and longitudinal evidence of increasing DMN within-network connectivity across development (Stevens et al. 2009; Supekar et al. 2010; Uddin et al. 2011; Sherman et al. 2014; Solé-Padullés et al. 2016). Importantly, segregation of the DMN, particularly among medial PFC regions, has been posited to be one developmental process by which internal-oriented functions mature (Sebastian et al. 2008; Supekar et al. 2010; Uddin 2010). Indeed, introspective processes such as social cognition and self-referential processing, are characterized by a prolonged developmental trajectory, beginning in later childhood and across adolescence (Sebastian et al. 2008). It is, therefore, possible that age-dependent changes in PFC regions might be evidence of DMN segregation across development that supports the maturity of introspective cognition.

Finally, it is worth noting that although many PFC regions displayed trajectories very much in alignment with their networks, most PFC regions remained stable in their topology across development. Given some evidence that hub regions, particularly frontal hubs, develop at different rates from non-hub regions, a secondary goal was to examine whether PFC regions with age-related effects displayed relatively higher hub properties in comparison to regions with stable topological trajectories. Although hub status was found to be lower in PFC regions of the DMN compared with all other networks, and the DAN lower in hub status than the FPN, our findings failed to show clear systematic differences in hubness between regions with age-dependent effects and regions of stable trajectories within a given network.

Therefore, while at least a subset of PFC regions appear to develop in ways that parallel their affiliated network, the mechanisms that facilitate age-related change in some regions but not others remains an open question in need of future research.

Cognition

Our findings show that PFC regions implicated in DMN segregation displayed broad relationships to cognition, predicting better performance in social cognition, complex cognition, and executive control. Notably, topology of DMN-linked PFC regions also predicted motor speed, suggesting that age-related effects of PFC topology are not specific to higher order cognition and, instead, may be important for more general processing functions that impact both basic and more complex processes. While there is a large literature delineating the role of the DMN in introspective functions, some evidence also suggests that DMN might play an indirect but important role in supporting general attentional demands by deactivating the DMN (potentially suppressing introspection) and concurrently activating control networks (Shulman et al. 2007 ; Anticevic et al. 2010; Satterthwaite et al. 2013b). Thus, in order to appropriately attend to the task at hand, it may be necessary to suppress introspective functions supported by the DMN. In this way, it is possible that both tasks requiring basic attentional demands and more complex attentional control may rely on the proper segregation of the DMN for optimal activation of task positive networks and suppression of task-negative (i.e., DMN) networks. Although speculative, this hypothesis is consistent with evidence of modifications in DMN segregation (i.e., increased network integration) during periods of mind wandering (Christoff et al. 2009; Smallwood et al. 2012), in part characterized by reductions in attention-directed cognition (Smallwood et al. 2008). Of note, PFC regions of the DAN and FPN were also found to predict executive control; however, these effects did not survive multiple comparison correction and should, therefore, be interpreted with caution.

Finally, we examined whether PFC topology of the DMN-mediated cognition and motor speed improvements with age. However, despite significant and independent relationships between age, PFC topology, and cognition, we did not find evidence that PFC topology mediated the relationship between age and cognitive maturity. One potential explanation for these findings is that PFC regions represent only one component of larger distributed networks (e.g., Power et al. 2011), in which other critical regions of a network are also expected to contribute to network segregation and integration to support cognitive development. Thus, while valuable in delineating the differential relationships that PFC regions show in facilitating network topology, the contributions of prefrontal regions in supporting cognitive maturity likely take place through interactions with other brain regions in the broader context of large-scale networks.

There are 2 key limitations worth emphasizing in the consideration of our findings. First, this dataset is cross-sectional, precluding the characterization of change over time within individuals. Although our findings are in strong agreement with existing longitudinal work examining network-level topological changes, future work using longitudinal, intra-individual designs will be needed to confirm whether topological age-related effects of distinct PFC regions, indeed, follow the shapes of diverging age-related differences suggested by our findings. Such designs may also be better equipped to more specifically characterize the ways in which PFC regions facilitate network

segregation and integration. Another limitation to consider is that the current study examined only a subset of ROIs (i.e., 28 seeds of 67 total seeds) within the PFC, with a focus largely placed on selecting ROIs on the basis of network affiliation, particularly canonical regions of a given network. In doing so, however, developmental trajectories for all possible PFC regions for each network were not studied and, to our knowledge, the trajectories of participation coefficient for PFC regions not included in the present study (i.e., 39 ROIs) have not been previously examined. Such a design inherently limits our ability to (1) identify other PFC regions that might be equally important in facilitating topological change at the network level and (2) comprehensively examine whether relative hub status within a network truly holds no bearing on age-related effects of PFC topology.

Additionally, an important consideration for future work will be to better understand variability of PFC functional connectivity at the individual level. A recent series of studies have shown that precision functional mapping—a data acquisition and analysis approach in which individuals are scanned repeatedly over multiple sessions—yields functional connectivity data that achieves excellent reliability. This allows the precise characterization of individual level functional connectivity (Braga and Buckner 2017; Gordon et al. 2017; Gratton et al. 2018a; Marek et al. 2018), exceeding the reliability observed with typical quantities of data (<10 min that are limited by relatively low signal-to-noise ratio (Laumann et al. 2015). A critical finding from precision mapping studies is that functional connectivity displays both common organizational principles across individuals, as well as, individual-specific features that are unresolvable in group-average data (Laumann et al. 2015; Gordon et al. 2017). These individual-specific features are particularly evident among higher order cognitive networks, with the PFC containing the greatest level of individual variability in functional connectivity and network organization compared with any other cortical region (Mueller et al. 2015; Gratton et al. 2018a). As a result, group average templates and large datasets with relatively smaller quantities of resting state data per subject, such as the current dataset, may have the effect of blurring individual-specific differences in PFC organization, with the potential to also obscure the detection of meaningful brain–behavior relationships (Finn et al. 2017). This is especially important to consider in the context of our study, which was able to measure common (average) developmental trajectories of PFC organization and functional connectivity across individuals, but limited in detecting individual-specific differences. As such, the future use of precision mapping to further delineate PFC development will be critical to capture individual-level variability in PFC network affiliation, changes in network topology, connectivity patterns, and relationships to cognition.

Conclusion

PFC regions systematically differ in their topological trajectories. Whereas PFC regions of the DAN, VAN, FPN, and DMN appear to aid network segregation, by strengthening within-network connections and reducing between-network connectivity, PFC regions of the CO/SN network plays a distinctive role in facilitating network integration by strengthening connectivity with a number of control and sensory networks. Importantly, these trajectories are largely consistent with developmental changes observed at the network level, suggesting that (1) topological trajectories across PFC regions systematically differ, largely on the basis of their network affiliation and (2) PFC regions play

differential roles in the development of network topology, representing important neural signatures of typical brain development. Trajectories of PFC regions of the DMN, in particular, appear to be related to global cognitive processing, though they did not emerge as a mechanistic link between age and cognitive maturity. Thus, while PFC topology does not appear to be a mechanism by which cognition improves across development, different PFC regions do appear to play critical roles in the development of network-level topology, which in turn, may support cognitive maturity.

Supplementary Material

Supplementary material is available at *Cerebral Cortex* online.

Notes

Any opinions, findings, and conclusions or recommendations expressed in this material are those of the author(s) and do not necessarily reflect the views of the National Science Foundation. *Conflict of Interest:* None declared.

References

Anticevic A, Repovs G, Shulman GL, Barch DM. 2010. When less is more: TPJ and default network deactivation during encoding predicts working memory performance. *NeuroImage*. 49(3), 2638–2648. doi: 10.1016/j.neuroimage.2009.11.008.

Baum GL, Ciric R, Roalf DR, Betzel RF, Moore TM, Shinohara RT et al. 2017. Modular segregation of structural brain networks supports the development of executive function in youth. *Curr Biol*. 27(11), 1561–1572.e8. doi: 10.1016/j.cub.2017.04.051.

Braga RM, Buckner RL. 2017. Parallel interdigitated distributed networks within the individual estimated by intrinsic functional connectivity. *Neuron*. 95(2), 457–471.e5. doi: 10.1016/j.neuron.2017.06.038.

Bressler SL, Menon V. 2010. Large-scale brain networks in cognition: emerging methods and principles. *Trends Cogn Sci*. 14(6), 277–290. doi: 10.1016/j.tics.2010.04.004.

Bunge S. A., Dudukovic N. M., Thomason M. E., Vaidya C. J. & Gabrieli J. D. E.. (2002). Immature Frontal Lobe Contributions to Cognitive Control in Children: Evidence from fMRI. *Neuron*. 33(2), 301–311. http://doi.org/10.1016/S0896-6273(01)00583-9.

Cao M, Wang JH, Dai ZJ, Cao XY, Jiang LL, Fan FM, He Y. 2014. Topological organization of the human brain functional connectome across the lifespan. *Dev Cogn Neurosci*. 7, 76–93. doi: 10.1016/j.dcn.2013.11.004.

Casey BJ, Tottenham N, Liston C, Durston S. 2005. Imaging the developing brain: what have we learned about cognitive development? *Trends Cogn Sci*. 9(3), 105–110. doi: 10.1016/j.tics.2005.01.011.

Christoff K, Gordon AM, Smallwood J, Smith R, Schooler JW. 2009. Experience sampling during fMRI reveals default network and executive system contributions to mind wandering. *Proc Natl Acad Sci*. 106(21), 8719–24. doi: 10.1073/pnas.0900234106.

Cole MW, Bassett DS, Power JD, Braver TS, Petersen SE. 2014. Intrinsic and task-evoked network architectures

of the human brain. *Neuron*. 83(1), 238–251. doi: 10.1016/j.neuron.2014.05.014.

Corbetta M. & Shulman G. L. (2002). Control of goal-directed and stimulus-driven attention in the brain. *Nature Reviews Neuroscience*, 3(3), 201–215. http://doi.org/10.1038/nrn755.

Cox RW, Chen G, Glen DR, Reynolds RC, Taylor PA. 2017. FMRI clustering in AFNI: false-positive rates Redux. *Brain Connect*. 7(3), 152–171. doi: 10.1089/brain.2016.0475.

Diamond A. 2009. Normal development of prefrontal cortex from birth to young adulthood: cognitive functions, anatomy, and biochemistry. In: *Principles of frontal lobe function*. (pp. 466–503). New York, NY, US: Oxford University Press. doi: 10.1093/acprof:oso/9780195134971.003.0029.

Diamond A. 2012. *Executive functions*. doi: 10.1146/annurev-psych-113011-143750.

Dixon ML, De La Vega A, Mills C, Andrews-Hanna J, Spreng RN, Cole MW, Christoff K. 2018. Heterogeneity within the frontoparietal control network and its relationship to the default and dorsal attention networks. *Proc Natl Acad Sci*. 115(7), E1598–E1607. doi: 10.1073/pnas.1715766115.

Dosenbach NUF, Fair DA, Cohen AL, Schlaggar BL, Petersen SE. 2008. A dual-networks architecture of top-down control. *Trends Cogn Sci*. 12(3):99–105. doi: 10.1016/j.tics.2008.01.001.

Dosenbach NUF, Fair DA, Miezin FM, Cohen AL, Wenger KK, Dosenbach RAT *et al*. 2007. Distinct brain networks for adaptive and stable task control in humans. *Proc Natl Acad Sci USA*. 104(26):11073–11078. doi: 10.1073/pnas.0704320104.

Eickhoff SB, Nichols TE, Laird AR, Hoffstaedter F, Amunts K, Fox PT *et al*. 2016. Behavior, sensitivity, and power of activation likelihood estimation characterized by massive empirical simulation. *NeuroImage*. 1–33. doi: 10.1016/j.neuroimage.2016.04.072.

Fair DA, Schlaggar BL, Cohen AL, Miezin FM, Dosenbach NUF, Wenger KK *et al*. 2007. A method for using blocked and event-related fMRI data to study "resting state" functional connectivity. *NeuroImage*. 35(1), 396–405. doi: 10.1016/j.neuroimage.2006.11.051.

Fan Y., Shi F., Smith J. K., Lin W., Gilmore J. H. & Shen D. (2011). Brain anatomical networks in early human brain development. *NeuroImage*, 54(3), 1862–1871. http://doi.org/10.1016/J.NEUROIMAGE.2010.07.025.

Farrant K, Uddin LQ. 2015. Asymmetric development of dorsal and ventral attention networks in the human brain. *Dev Cogn Neurosci*. 12, 165–174. doi: 10.1016/j.dcn.2015.02.001.

Finn ES, Scheinost D, Finn DM, Shen X, Papademetris X, Constable RT. 2017. Can brain state be manipulated to emphasize individual differences in functional connectivity? *NeuroImage*. 160, 140–151. doi: 10.1016/j.neuroimage.2017.03.064.

Fischl B, Salat DH, Busa E, Albert M, Dieterich M, Haselgrove C *et al*. 2002. Whole brain segmentation: automated labeling of neuroanatomical structures in the human brain. *Neuron*. 33(3), 341–355. doi: 10.1016/S0896-6273(02)00569-X.

Fox MD, Raichle ME. 2007. Spontaneous fluctuations in brain activity observed with functional magnetic resonance imaging. *Nat Rev Neurosci*. doi: 10.1038/nrn2201.

Fox MD, Snyder AZ, Zacks JM, Raichle ME. 2006. Coherent spontaneous activity accounts for trial-to-trial variability in human evoked brain responses. *Nat Neurosci*. 9(1), 23–25. doi: 10.1038/nn1616.

Friston KJ, Fletcher P, Josephs O, Holmes A, Rugg MD, Turner R. 1998. Event-related fMRI: characterizing differential responses. *NeuroImage*. 7(1), 30–40. doi: 10.1006/nimg.1997.0306.

Gee DG, Humphreys KL, Flannery J, Goff B, Telzer EH, Shapiro M *et al*. 2013. A developmental shift from positive to negative connectivity in human amygdala—prefrontal circuitry. *J Neurosci*. 33(10):4584–4593. doi: 10.1523/JNEUROSCI.3446-12.2013.

Giedd JN, Blumenthal J, Jeffries NO, Castellanos FX, Liu H, Zijdenbos A *et al*. 1999. Brain development during childhood and adolescence: a longitudinal MRI study. *Nat Neurosci*. 2, 861–863. doi: 10.1038/13158.

Gogtay N, Giedd JN, Lusk L, Hayashi KM, Greenstein D, Vaituzis AC *et al*. 2004. Dynamic mapping of human cortical development during childhood through early adulthood. *Proc Natl Acad Sci*. 98(20), 11650–11655. doi: 10.1073/pnas.0402680101.

Gordon EM, Laumann TO, Gilmore AW, Newbold DJ, Greene DJ, Berg JJ *et al*. 2017. Precision functional mapping of individual human brains. *Neuron*. doi: 10.1016/j.neuron.2017.07.011.

Gratton C, Laumann TO, Nielsen AN, Greene DJ, Gordon EM, Gilmore AW *et al*. 2018a. Functional brain networks are dominated by stable group and individual factors, not cognitive or daily variation. *Neuron*. 98(2), 439–452.e5. doi: 10.1016/j.neuron.2018.03.035.

Gratton C, Sun H, Petersen SE. 2018b. Control networks and hubs. *Psychophysiology*. Blackwell Publishing Inc. doi: 10.1111/psyp.13032.

Grayson DS, Fair DA. 2017. Development of large-scale functional networks from birth to adulthood: a guide to the neuroimaging literature. *NeuroImage*. 160, 15–31. doi: 10.1016/j.neuroimage.2017.01.079.

Grayson DS, Ray S, Carpenter S, Iyer S, Dias TGC, Stevens C, Fair DA. 2014. Structural and functional rich club organization of the brain in children and adults. *PLoS One*. 9(2), e88297. 10.1109/VR.2017.7892250.

Gu S, Satterthwaite TD, Medaglia JD, Yang M, Gur RE, Gur RC, Bassett DS. 2015. Emergence of system roles in normative neurodevelopment. *Proc Natl Acad Sci*. 112(44), 13681–13686. doi: 10.1073/pnas.1502829112.

Kanemura H, Aihara M, Aoki S, Araki T, Nakazawa S. 2003. Development of the prefrontal lobe in infants and children: a three-dimensional magnetic resonance volumetric study. *Brain Dev*. 25(3), 195–199. doi: 10.1016/S0387-7604(02)00214-0.

Krawczyk D. C., Michelle McClelland M. & Donovan C. M. (2011). A hierarchy for relational reasoning in the prefrontal cortex. *Cortex*, 47(5), 588–597. http://doi.org/10.1016/J.CORTEX.2010.04.008.

Laumann TO, Gordon EM, Adeyemo B, Snyder AZ, Joo SJ, Chen MY *et al*. 2015. Functional system and areal organization of a highly sampled individual human brain. *Neuron*. 87(3), 657–670. doi: 10.1016/j.neuron.2015.06.037.

Lee K, Bull R, Ho RMH. 2013. Developmental changes in executive functioning. *Child Dev*. 84(6), 1933–1953. doi: 10.1111/cdev.12096.

Luking KR, Repovs G, Belden AC, Gaffrey MS, Botteron KN, Luby JL, Barch DM. 2011. Functional connectivity of the amygdala in early-childhood-onset depression. *J Am Acad Child Adolesc Psychiatry*. 50(10):1027–1041.e3. doi: 10.1016/j.jaac.2011.07.019.

Luna B, Thulborn KR, Munoz DP, Merriam EP, Garver KE, Minshew NJ *et al*. 2001. Maturation of widely distributed brain function subserves cognitive development. *NeuroImage*. 13(5), 786–793. doi: 10.1006/nimg.2000.0743.

Marek S, Dosenbach NUF. 2018. The frontoparietal network: function, electrophysiology, and importance of individual precision mapping. *Dialogues Clin Neurosci*.

Marek S, Hwang K, Foran W, Hallquist MN, Luna B. 2015. The contribution of network organization and integration to the development of cognitive control. *PLoS Biol*. 13(12). doi: 10.1371/journal.pbio.1002328.

Marek S, Siegel JS, Gordon EM, Raut RV, Gratton C, Newbold DJ et al. 2018. Spatial and temporal organization of the individual human cerebellum. *Neuron*. 100(4), 977–993.e7. doi: 10.1016/j.neuron.2018.10.010.

Matsui M, Tanaka C, Niu L, Noguchi K, Bilker WB, Wierzbicki M, Gur RC. 2016. Age-related volumetric changes of prefrontal gray and white matter from healthy infancy to adulthood. *Int J Clin Exp Neurol*. 4(1):1–8. doi: 10.12691/IJCEN-4-1-1.

McAvoy MP, Corbetta M, Shulman GL, Tansy AP, Cowan MC, Astafiev SV, d'Avossa G. 2006. Quantitative analysis of attention and detection signals during visual search. *J Neurophysiol*. doi: 10.1152/jn.00343.2003.

Meunier D., Achard S., Morcom A. & Bullmore E. (2009). Age-related changes in modular organization of human brain functional networks. *NeuroImage*, 44(3), 715–723. http://doi.org/10.1016/j.neuroimage.2008.09.062.

Mohr H, Wolfensteller U, Betzel RF, Mišić B, Sporns O, Richiardi J, Ruge H. 2016. Integration and segregation of large-scale brain networks during short-term task automatization. *Nat Commun*. doi: 10.1038/ncomms13217.

Moore TM, Reise SP, Gur RE, Hakonarson H, Gur RC. 2015. Psychometric properties of the penn computerized neurocognitive battery. *Neuropsychology*. doi: 10.1037/neu0000093.

Mueller S, Wang D, Fox MD, Pan R, Lu J, Li K et al. 2015. Reliability correction for functional connectivity: theory and implementation. *Hum Brain Mapp*. 36(11):4664–4680. doi: 10.1002/hbm.22947.

Nakamura T, Hillary FG, Biswal BB. 2009. Resting network plasticity following brain injury. *PLoS One*. 4(12). doi: 10.1371/journal.pone.0008220.

Ojemann JG, Akbudak E, Snyder AZ, McKinstry RC, Raichle ME, Conturo TE. 1997. Anatomic localization and quantitative analysis of gradient refocused echo-planar fMRI susceptibility artifacts. *NeuroImage*. 6(3), 156–167. doi: 10.1006/nimg.1997.0289.

Ordaz SJ, Foran W, Velanova K, Luna B. 2013. Longitudinal growth curves of brain function underlying inhibitory control through adolescence. *J Neurosci*. 33(46):18109–18124. doi: 10.1523/JNEUROSCI.1741-13.2013.

Petersen SE, Posner MI. 2012. The attention system of the human brain: 20 years after. *Annu Rev Neurosci*. 35(1), 73–89. doi: 10.1146/annurev-neuro-062111-150525.

Petrican R, Taylor MJ, Grady CL. 2017. Trajectories of brain system maturation from childhood to older adulthood: implications for lifespan cognitive functioning. *NeuroImage*. 163, 125–149. doi: 10.1016/j.neuroimage.2017.09.025.

Posner MI, Rothbart MK, Rueda MR. 2013. Developing attention and self-regulation in infancy and childhood. In: *Neural Circuit Development and Function in the Heathy and Diseased Brain*. (pp. 395–411). Elsevier Inc. doi: 10.1016/B978-0-12-397267-5.00059-5.

Power J. D., Fair D. A., Schlaggar B. L. & Petersen S. E. (2010). The Development of Human Functional Brain Networks. *Neuron*, 67(5), 735–748. http://doi.org/10.1016/J.NEURON.2010.08.017.

Power JD, Cohen AL, Nelson SSM, Wig GS, Barnes KA, Church JA et al. 2011. Functional network organization of the human brain. *Neuron*. 72(4):665–678. doi: 10.1016/j.neuron.2011.09.006.Functional.

Power J. D. & Petersen S. E. (2013, April). Control-related systems in the human brain. *Current Opinion in Neurobiology*. http://doi.org/10.1016/j.conb.2012.12.009.

Power JD, Mitra A, Laumann TO, Snyder AZ, Schlaggar BL, Petersen SE. 2014. NeuroImage methods to detect, characterize, and remove motion artifact in resting state fMRI. *NeuroImage*. 84:320–341. doi: 10.1016/j.neuroimage.2013.08.048.

Power JD, Schlaggar BL, Petersen SE. 2015. Recent progress and outstanding issues in motion correction in resting state fMRI. *NeuroImage*. 105:536–551. doi: 10.1016/j.neuroimage.2014.10.044.

Powers. 2010. Evidence for hubs in human functional brain networks. 48(Suppl 2):1–6. doi: 10.1097/MPG.0b013e3181a15ae8.Screening.

Ptak R, Schnider A, Fellrath J. 2017. The dorsal Frontoparietal network: a Core system for emulated action. *Trends Cogn Sci*. Elsevier Ltd. doi: 10.1016/j.tics.2017.05.002.

Raichle ME. 2015. The brain's default mode network. *Annu Rev Neurosci*. 38(1), 433–447. doi: 10.1146/annurev-neuro-071013-014030.

Rosseel Y. 2012. Lavaan: an R package for structural equation modeling. *J Stat Softw*. doi: 10.18637/jss.v048.i02.

Rubia K, Smith AB, Woolley J, Nosarti C, Heyman I, Taylor E, Brammer M. 2006. Progressive increase of frontostriatal brain activation from childhood to adulthood during event-related tasks of cognitive control. *Hum Brain Mapp*. 27(12), 973–993. doi: 10.1002/hbm.20237.

Rubinov M, Sporns O. 2010. Complex network measures of brain connectivity: uses and interpretations. *NeuroImage*. 52(3):1059–1069. doi: 10.1016/j.neuroimage.2009.10.003.

Sadaghiani S, D'Esposito M. 2015. Functional characterization of the cingulo-opercular network in the maintenance of tonic alertness. *Cereb Cortex*. 25(9), 2763–2773. doi: 10.1093/cercor/bhu072.

Satterthwaite TD, Connolly JJ, Ruparel K, Calkins ME, Jackson C, Elliott MA et al. 2016. The Philadelphia neurodevelopmental cohort: a publicly available resource for the study of normal and abnormal brain development in youth. *NeuroImage*. 124:1115–1119. doi: 10.1016/j.neuroimage.2015.03.056.

Satterthwaite TD, Wolf DH, Erus G, Ruparel K, Elliott MA, Gennatas ED et al. 2013a. Functional maturation of the executive system during adolescence. *J Neurosci*. 33(41), 16249–16261. doi: 10.1523/jneurosci.2345-13.2013.

Satterthwaite TD, Wolf DH, Roalf DR, Ruparel K, Erus G, Vandekar S et al. 2015. Linked sex differences in cognition and functional connectivity in youth. *Cereb Cortex*. 25(9), 2383–2394. doi: 10.1093/cercor/bhu036.

Satterthwaite TD, Wolf DH, Ruparel K, Erus G, Elliott MA, Eickhoff SB, Gur RC. 2013b. Heterogeneous impact of motion on fundamental patterns of developmental changes in functional connectivity during youth. *NeuroImage*. doi: 10.1016/j.neuroimage.2013.06.045.

Sebastian C, Burnett S, Blakemore SJ. 2008. Development of the self-concept during adolescence. *Trends Cogn Sci*. doi: 10.1016/j.tics.2008.07.008.

Sheffield JM, Repovs G, Harms MP, Carter CS, Gold JM, MacDonald AW, Barch DM. 2015. Fronto-parietal and cingulo-opercular network integrity and cognition in health and schizophrenia. *Neuropsychologia*. 73, 82–93. doi: 10.1016/j.neuropsychologia.2015.05.006.

Sherman LE, Rudie JD, Pfeifer JH, Masten CL, McNealy K, Dapretto M. 2014. Development of the default mode and central execu-

tive networks across early adolescence: a longitudinal study. *Dev Cogn Neurosci*. 10, 148–159. doi: 10.1016/j.dcn.2014.08.002.

Shulman GL, Astafiev SV, McAvoy MP, D'Avossa G, Corbetta M. 2007. Right TPJ deactivation during visual search: functional significance and support for a filter hypothesis. *Cereb Cortex*. 17(11), 2625–2633. doi: 10.1093/cercor/bhl170.

Smallwood J, Brown K, Baird B, Schooler JW. 2012. Cooperation between the default mode network and the frontal-parietal network in the production of an internal train of thought. *Brain Res*. doi: 10.1016/j.brainres.2011.03.072.

Smallwood J, McSpadden M, Schooler JW. 2008. When attention matters: the curious incident of the wandering mind. *Mem Cogn*. 36(6), 1144–1150. doi: 10.3758/MC.36.6.1144.

Solé-Padullés C, Castro-Fornieles J, De La Serna E, Calvo R, Baeza I, Moya J et al. 2016. Intrinsic connectivity networks from childhood to late adolescence: effects of age and sex. *Dev Cogn Neurosci*. 17:35–44. doi: 10.1016/j.dcn.2015.11.004.

Sowell ER. 2004. Longitudinal mapping of cortical thickness and brain growth in normal children. *J Neurosci*. 24(38), 8223–8231. doi: 10.1109/CDC.2017.8264670.

Spencer-Smith M, Anderson V. 2009. Healthy and abnormal development of the prefrontal cortex. *Dev Neurorehabil*. doi: 10.3109/17518420903090701.

Spreng RN, Sepulcre J, Turner GR, Stevens WD, Schacter DL. 2013. Intrinsic architecture underlying the relations among the default, dorsal attention, and frontoparietal control networks of the human brain. *J Cogn Neurosci*. 25(1), 74–86. doi: 10.1162/jocn_a_00281.

Stevens MC, Pearlson GD, Calhoun VD. 2009. Changes in the interaction of resting-state neural networks from adolescence to adulthood. *Hum Brain Mapp*. 30(8), 2356–2366. doi: 10.1002/hbm.20673.

Supekar K, Uddin LQ, Prater K, Amin H, Greicius MD, Menon V. 2010. Development of functional and structural connectivity within the default mode network in young children. *NeuroImage*. 52(1), 290–301. doi: 10.1016/j.neuroimage.2010.04.009.

Swagerman SC, De Geus EJC, Kan KJ, Van Bergen E, Nieuwboer HA, Koenis MMG et al. 2016. The computerized neurocognitive battery: validation, aging effects, and heritability across cognitive domains. *Neuropsychology*. 30(1), 53–64. doi: 10.1037/neu0000248.

Sylvester CM, Barch DM, Corbetta M, Power JD, Schlaggar BL, Luby JL. 2013. Resting state functional connectivity of the ventral attention network in children with a history of depression or anxiety. *J Am Acad Child Adolesc Psychiatry*. 52(12):1326–1336.e5. doi: 10.1016/j.jaac.2013.10.001.

Szczepanski SM, Pinsk MA, Douglas MM, Kastner S, Saalmann YB. 2013. Functional and structural architecture of the human dorsal frontoparietal attention network. *Proc Natl Acad Sci*. 110(39), 15806–15811. doi: 10.1073/pnas.1313903110.

Tamm L, Menon V, Reiss AL. 2002. Maturation of brain function associated with response inhibition. *J Am Acad Child Adolesc Psychiatry*. 41(10), 1231–1238. doi: 10.1097/00004583-200210000-00013.

Tamnes CK, Herting MM, Goddings A-L, Meuwese R, Blakemore S-J, Dahl RE et al. 2017. Development of the cerebral cortex across adolescence: a multisample study of interrelated longitudinal changes in cortical volume, surface area, and thickness. *J Neurosci*. 37(12):3402–3412. doi: 10.1523/JNEUROSCI.3302-16.2017.

Todd JJ, Fougnie D, Marois R. 2005. Visual short-term memory load suppresses temporo-parietal junction activity and induces inattentional blindness. *Psychol Sci*. 16(12), 965–972. doi: 10.1111/j.1467-9280.2005.01645.x.

Uddin LQ. 2010. Typical and atypical development of functional human brain networks: insights from resting-state fMRI. *Front Syst Neurosci*. doi: 10.3389/fnsys.2010.00021.

Uddin L, Supekar K, Ryali S, Menon V. 2011. Dynamic reconfiguration of structural and functional connectivity across core neurocognitive brain networks with development. *J Neurosci*. 31(50):18578–18589. doi: 10.1523/JNEUROSCI.4465-11.2011.Dynamic.

Velanova K, Wheeler ME, Luna B. 2008. Maturational changes in anterior cingulate and frontoparietal recruitment support the development of error processing and inhibitory control. *Cereb Cortex*. 18(11), 2505–2522. doi: 10.1093/cercor/bhn012.

Vossel S, Geng JJ, Fink GR. 2014. Dorsal and ventral attention systems: distinct neural circuits but collaborative roles. *Neuroscientist*. 20(2), 150–159. doi: 10.1177/1073858413494269.

Wallis G, Stokes M, Cousijn H, Woolrich M, Nobre AC. 2015. Frontoparietal and cingulo-opercular networks play dissociable roles in control of working memory. *J Cogn Neurosci*. 27(10), 2019–2034. doi: 10.1162/jocn_a_00838.

Waltz J. A., Knowlton B. J., Holyoak K. J., Boone K. B., Mishkin F. S., de Menezes Santos M., Miller B. L. (1999). A system for relational reasoning in human prefrontal cortex. *Psychological Science*, 10(2), 119–125. http://doi.org/10.1111/1467-9280.00118.

Wang L, LaBar KS, Smoski M, Rosenthal MZ, Dolcos F, Lynch TR et al. 2008. Prefrontal mechanisms for executive control over emotional distraction are altered in major depression. *Psychiatry Res Neuroimaging*. 163(2):143–155. doi: 10.1016/j.pscychresns.2007.10.004.

Wood SN. 2017. *Generalized additive models: an introduction with R.* 2nd edn. doi: 10.1201/9781315370279.

Wu K, Taki Y, Sato K, Hashizume H, Sassa Y, Takeuchi H et al. 2013. Topological organization of functional brain networks in healthy children: differences in relation to age, sex, and intelligence. *PLoS One*. 8(2). doi: 10.1371/journal.pone.0055347.

Yeo BTT, Krienen FM, Sepulcre J, Sabuncu MR, Lashkari D, Hollinshead M et al. 2011. The Organization of the Human Cerebral Cortex Estimated by functional connectivity. *J Neurophysiol*. doi: 10.1152/jn.00338.2011.